INTERNATIONAL JOURNAL FOR NUMERICAL METHODS IN FLUIDS
Int. J. Numer. Meth. Fluids 2005; **49**:569–582
Published online 9 June 2005 in Wiley InterScience (www.interscience.wiley.com). DOI: 10.1002/fld.1013

Numerical investigation of natural convection inside an inclined parallel-walled channel

S. A. M. Said*,†, M. A. Habib‡, H. M. Badr§ and S. Anwar¶

Mechanical Engineering Department, King Fahd University of Petroleum and Minerals, Dhahran 31261, Saudi Arabia

SUMMARY

Steady two-dimensional natural convection in an inclined parallel-walled channel was investigated numerically. The full elliptic forms of conservation equations were solved together and the velocity vectors, temperature contours and local and average Nusselt number distribution were obtained. The comparisons of local and average Nusselt number with published experimental and numerical results indicate very good agreement. Results are presented for a single aspect ratio, $L/b = 24$, over the range of Rayleigh number of 3–1000 and angle of inclination 0–90°. The results indicate that the overall channel average Nusselt number is reduced as the inclination angle is increased. Significant reductions in the overall Nusselt number are exhibited at high angle of channel inclination. Copyright © 2005 John Wiley & Sons, Ltd.

KEY WORDS: natural convection; inclined; channel

1. INTRODUCTION

Laminar natural convection flows are of interest in a number of engineering applications such as computers, electronic cooling, solar collection systems and building energy systems. Heated channel configurations, which are cooled by natural convection, are found in electronic cabinets containing circuit boards, which are aligned in vertical or inclined arrays, with channels formed between each of the two boards. Many diverse flow configurations are of interest in this regard. The case where the channel walls are parallel and vertical have been investigated theoretically as well as experimentally. Several investigators [1–10] have made contributions

*Correspondence to: S. A. M. Said, Mechanical Engineering Department, King Fahd University of Petroleum and Minerals, Dhahran 31261, Saudi Arabia.
†E-mail: samsaid@kfupm.edu.sa
‡E-mail: mahabib@kfupm.edu.sa
§E-mail: badrhm@kfupm.edu.sa
¶E-mail: sohail@kfupm.edu.sa

Contract/grant sponsor: King Fahd University of Petroleum and Minerals

Received 31 January 2004
Revised 5 May 2005
Accepted 10 May 2005

to the literature on the subject where the channel walls are parallel and vertical and many aspects of flows are now well understood.

In comparison with vertical channels, the inclined channel has received little attention. Recent contributions to the literature have been made by Azevedo and Sparrow [11], Hajjai and Warek [12], Straatman *et al.* [13], Onur and Aktas [14], Baskaya *et al.* [15], Bianco *et al.* [16] and Manca *et al.* [17]. Azevedo and Sparrow [11] carried out experiments on an inclined isothermal channel using water as the working fluid. They investigated three modes of heating in which either both walls were heated, or only the top wall only was heated or only the bottom wall was heated. Hajjai and Worek [12] analysed fully developed, combined, natural convection heat and mass transfer in an inclined channel using air as the working fluid. For the case of fully developed flow, close form expressions for the velocity, temperature and mass fraction profiles, and the Nusselt and Shroud numbers were obtained. Straatmen *et al.* [13] studied the effects of inclining an isothermal, parallel-walled channel on the local heat flux distribution along the walls.

Onur and Aktas [14] studied experimentally the effect of plate spacing and the inclination angle on air natural convection between inclined parallel plates in which the upper plate was heated isothermally whereas the lower plate was insulated. Experiments were performed for a plate inclination of 0°, 30° and 45° with respect to the vertical position. The results indicated that both the plate spacing and inclination influence the heat transfer rate.

Baskaya *et al.* [15] studied the numerical effects of the channel width and inclination on laminar air natural convection between asymmetrically heated parallel plates. The upper plate was isothermally heated while the lower plate was passively heated by the upper one. They observed that the channel width and inclination influence the overall heat transfer rate. Bianco *et al.* [16] described in a review article experimental and numerical studies in symmetrically and asymmetrically inclined channels. They considered utterly as well as discretely heated channel walls. The effects of the channel width, inclination angle, walls emissivity, the dissipated heat flux, the number and position of the discrete heat source along the walls were reported.

Manca *et al.* [17] studied experimentally the effect on air natural convection of the distance between an inclined discretely heated plate and a parallel shroud below. Several inclination angles were tested. The results indicated that for angles not greater than 85°, increasing the distance between walls does not reduce the wall temperature whereas for angles greater than 85° there is an opposite tendency.

The present study concerns a numerical investigation of laminar natural convection in a parallel-walled channel inclined with respect to gravity. The study covers a wide range of angles of inclination $0° \leqslant \theta \leqslant 90°$ and Rayleigh numbers $3 \leqslant Ra \leqslant 1000$.

2. PROBLEM FORMULATION

The present study considers the steady state, laminar, incompressible, two-dimensional natural convection flow of air (Newtonian fluid) that occurs in an inclined parallel-walled channel as shown in Figure 1. All the thermophysical properties are assumed to be constant, except for density in the buoyancy term that can be adequately modelled by the Boussinesq approximation [18] and that compression work, viscous dissipation and radiative transport are negligibly

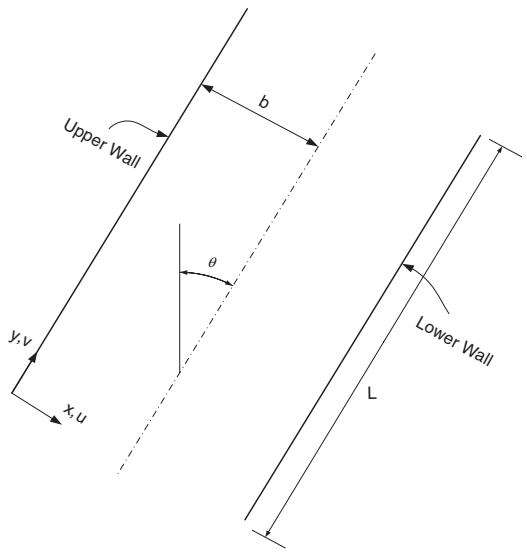

Figure 1. Flow geometry.

small. Thus, the governing equations are as follows:
Conservation of mass:

$$\frac{\partial u}{\partial x}+\frac{\partial v}{\partial y}=0 \tag{1}$$

Conservation of momentum:

$$u\frac{\partial u}{\partial x}+v\frac{\partial u}{\partial y}=-\frac{1}{\rho}\frac{\partial P}{\partial x}+\upsilon\left(\frac{\partial^2 u}{\partial x^2}+\frac{\partial^2 u}{\partial y^2}\right)+g\sin\theta\beta(T-T_0) \tag{2}$$

$$u\frac{\partial v}{\partial x}+v\frac{\partial v}{\partial y}=-\frac{1}{\rho}\frac{\partial P}{\partial y}+\upsilon\left(\frac{\partial^2 v}{\partial x^2}+\frac{\partial^2 v}{\partial y^2}\right)+g\cos\theta\beta(T-T_0) \tag{3}$$

Conservation of energy:

$$(\rho C_p)\left(u\frac{\partial T}{\partial x}+v\frac{\partial T}{\partial y}\right)=k\left(\frac{\partial^2 T}{\partial x^2}+\frac{\partial^2 T}{\partial y^2}\right) \tag{4}$$

where u and v are the velocity components in the x and y directions, T the temperature, P the 'motion pressure' (defined as the channel to ambient pressure difference), g the magnitude of the acceleration due to gravity, $\rho, \upsilon, \beta, C_p$ and k are, respectively, the fluid density, kinematic viscosity, coefficient of thermal expansion, constant pressure specific heat and thermal conductivity of air all evaluated at some reference temperature T_0. The boundary conditions corresponding to Equations (1)–(4) are given as

$$\begin{matrix} u=v=0 \\ T=T_{\mathrm{W}} \end{matrix}, \quad \text{for } 0\leqslant y\leqslant L,\ x=0 \tag{5}$$

$$\begin{matrix} u = v = 0 \\ T = T_W \end{matrix}, \quad \text{for } 0 \leqslant y \leqslant L,\ x = 2b \tag{6}$$

$$\begin{matrix} P = P_O \\ T = T_O \end{matrix}, \quad \text{for } y = 0 \tag{7}$$

$$P = P_O, \quad \text{for } y = L \tag{8}$$

At the inlet, the total pressure (p_s) is specified as ambient pressure. The inlet total pressure and static pressure, p_s, are related to the inlet velocity via Bernoulli's equation

$$p_O = p_s + \tfrac{1}{2}\rho v^2 \tag{9}$$

With the resulting velocity magnitude and the flow direction vector assigned at the inlet, the velocity components can be computed. The inlet mass flow rate and fluxes of momentum, energy, and species can then be computed as

$$\dot{m} = \int \rho v \, \mathrm{d}A \tag{10}$$

Only the velocity component normal to the control volume face contributes to the inlet mass flow rate. Density at the inlet plane is computed using Boussinesq approximation.

At the outlet, FLUENT uses the boundary condition ambient pressure as the static pressure p_s of the fluid and extrapolates all other conditions from the interior of the domain.

Computations were carried out for air ($Pr = 0.707$). The plates were maintained at a constant temperate T_W above the ambient T_O.

3. NUMERICAL SOLUTION

In the present study, the numerical solutions were carried out using the general purpose computer code FLUENT designed for the solution of incompressible fluid dynamic problems. The computational scheme that is used by Fluent Inc. [19] is based on the finite volume discretization method, which was described in sufficient detail by Patankar [20] and Versteegh and Malalasekera [21]. FLUENT uses SIMPLE algorithm [22] for pressure–velocity coupling. Choudhury [23] has reported fluid flow and heat transfer calculation using FLUENT for two benchmark problems. One of them was laminar natural convection. The FLUENT results were in close agreement with experimental measurements.

4. RESULTS AND DISCUSSION

Numerical results were obtained for uniform wall temperature conditions in an inclined parallel-walled channel. The channel was investigated for a single aspect ratio, $L/b = 24$, over the range $3 \leqslant Ra \leqslant 1000$, $0^\circ \leqslant \theta \leqslant 90^\circ$. Typical local heat transfer coefficients and average Nusselt number ($\overline{Nu}$) calculations were carried out. The results of these calculations are presented graphically.

The first set of results pertains to the grid independency test. Sequences of calculations at an increasing grid density were performed for the vertical channel. These calculations included the influence of mesh sizes of 25×100, 50×100, 50×200 and 100×300 on the mean vertical velocity at section $y/L = 0.77$. The results of these calculations are shown in Figure 2. The

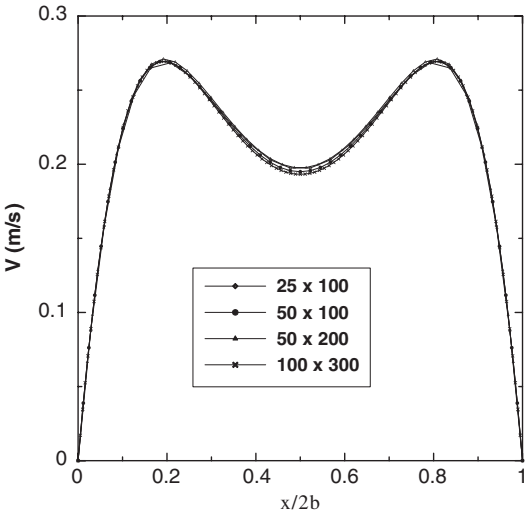

Figure 2. Grid independence test.

results indicate that the maximum numerical error in the mean velocity is reduced from 0.4 to 0.14% as the mesh is refined from 50×100 to 50×200 and from 50×200 to 100×300. A mesh size of 50×200 was adopted for the present numerical calculations.

The second set of results pertains to the validation of the numerical code used in carrying out the present numerical solutions. The comparison is conducted for a vertical channel with uniform wall temperature boundary condition. Figure 3(a) shows a comparison of the present numerical results for the local Nusselt number with similar experimental results by Wirtz and Haag [6] and similar numerical results by Naylor *et al.* [7]. The comparison is for the same Rayleigh number (3.11) and aspect ratio ($L/b = 24$). The present results for the local Nusselt number are in better agreement with the experimental ones as shown in Figure 3(a). A comparison of the average Nusselt number ($\overline{Nu}$) with experimental results by Elenbaas [1] and numerical results by Naylor *et al.* [7] for different Rayleigh number is shown in Figure 3(b) and Table I. Good agreement between the present results and similar ones reported in the literature is indicated by Figure 3(b).

The third set of results pertains to velocity vectors and velocity contours. Figure 4(a) shows the velocity vector plot for a 60° inclination angle. The results indicate that no reverse flow regions occur for inclination angles of up to $\theta = 60°$. Figure 4(b) shows velocity contours for a 60° inclination angle. It indicates a negligible velocity gradient along the centreline and high velocity gradients close to the upper and lower walls. The figure also indicates that the velocity contours exhibit symmetry around the centreline. A slight deviation of this symmetry is indicated at the exit section. This is attributed to the component of momentum towards the upper wall near the exit section. The same trend of symmetry is indicated by the temperature contours. Since all inclination angles less than or equal to 60° exhibit the same trend, the velocity vector plots for these inclination angles are not shown.

The corresponding velocity vector and velocity contours for the angle of inclination of 80° are shown in Figures 5 and 6 for the same modified Rayleigh number of 190. Figure 5

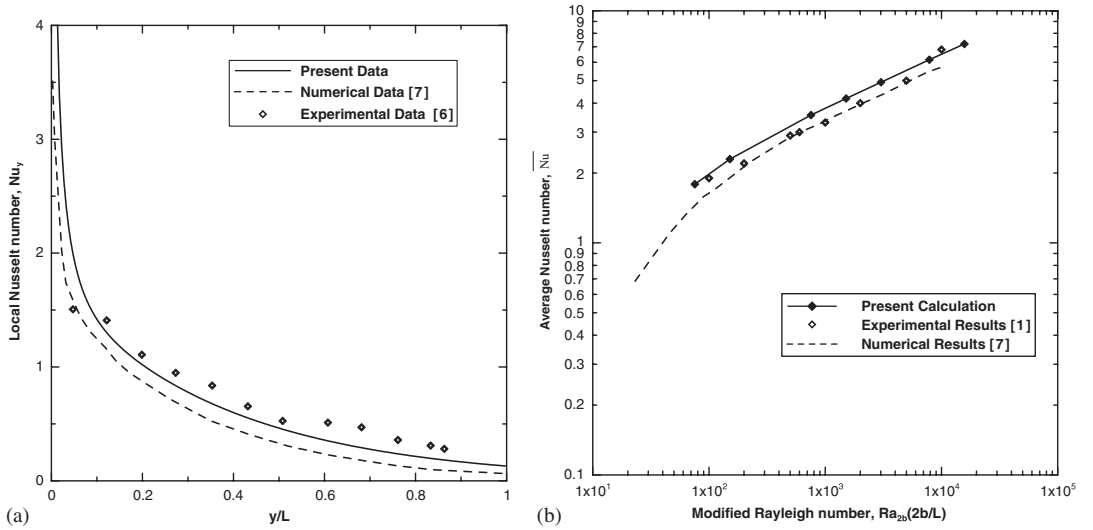

Figure 3. (a) Comparison of local Nusselt number distribution with experimental data of Wirtz and Haag [6] and Numerical data of Naylor *et al.* [7] for a vertical channel; and (b) comparison of average Nusselt number results with experimental data of Elenbass [1] and numerical data of Naylor *et al.* [7] for a vertical channel.

Table I. Comparison of present numerical results with experimental [1] and numerical [7] results.

Present calculation	$Ra_{2b}(2b/L)$	5	9.5	50	95	190	491.6	983.3
	$\overline{Nu}$	0.8945	1.1476	1.7765	2.094	2.4603	3.075	3.5973
Elenbass [1]	$Ra_{2b}(2b/L)$	6	10	50	100	200	500	1000
	$\overline{Nu}$	0.25	0.4	1.15	1.9	2.2	2.9	3.3
Naylor *et al.* [7]	$Ra_{2b}(2b/L)$	3.9289	7.1089	55.09161	69.466	194.9651	472.44	661.4115
	$\overline{Nu}$	0.660207	0.854028	1.62435	1.7233	2.18032	2.721	2.882919

indicates a reverse flow region in the vicinity of the lower plate close to the exit section. It shows a dramatic change in the velocity vector pattern at $\theta = 80°$ in comparison with that of $\theta = 60°$. The velocity pattern exhibits higher velocity gradients close to the upper wall in the vicinity of the channel inlet. In the vicinity of the channel exit, the flow moves upward, causing a higher velocity gradient close to the upper wall. A similar trend of temperature pattern as in the case of $\theta = 60°$ is observed for $\theta = 80°$ but with higher rates of temperature increase as the flow moves towards the channel exit. Thus, higher rates of thermal diffusion occur as the inclination angle increases.

The fourth set of results pertains to the local Nusselt number for three inclination angles. Figure 7 shows the variation of the local Nusselt number over each wall for inclination angles of 30°, 60° and 80° for $Ra' = 190$. As can be seen, the local Nusselt number decreases along

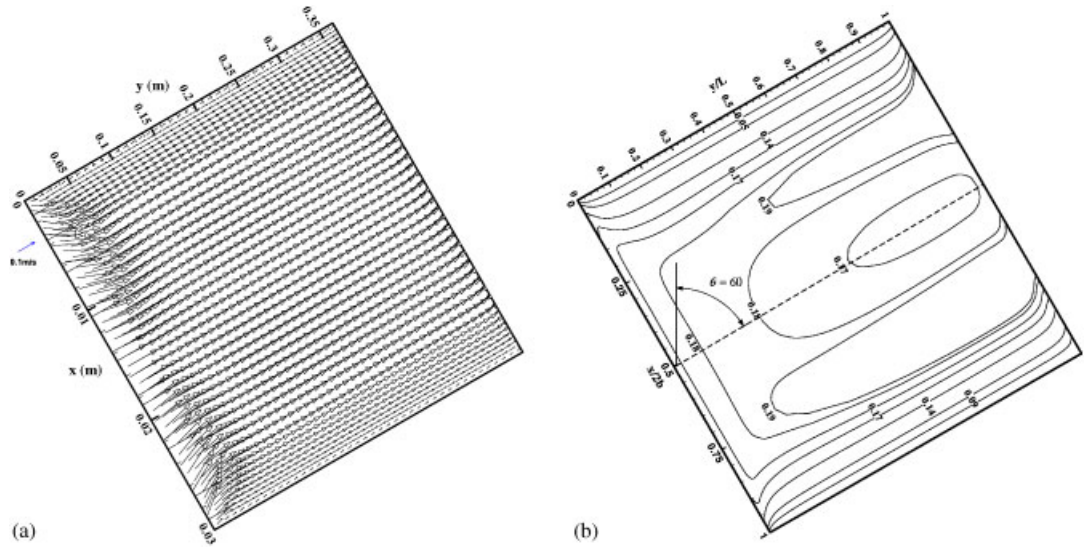

Figure 4. (a) Velocity vectors for 60° inclination angle at $Ra' = 190$; and (b) velocity contours for 60° inclination angle for $Ra' = 190$. All velocities are in m/s.

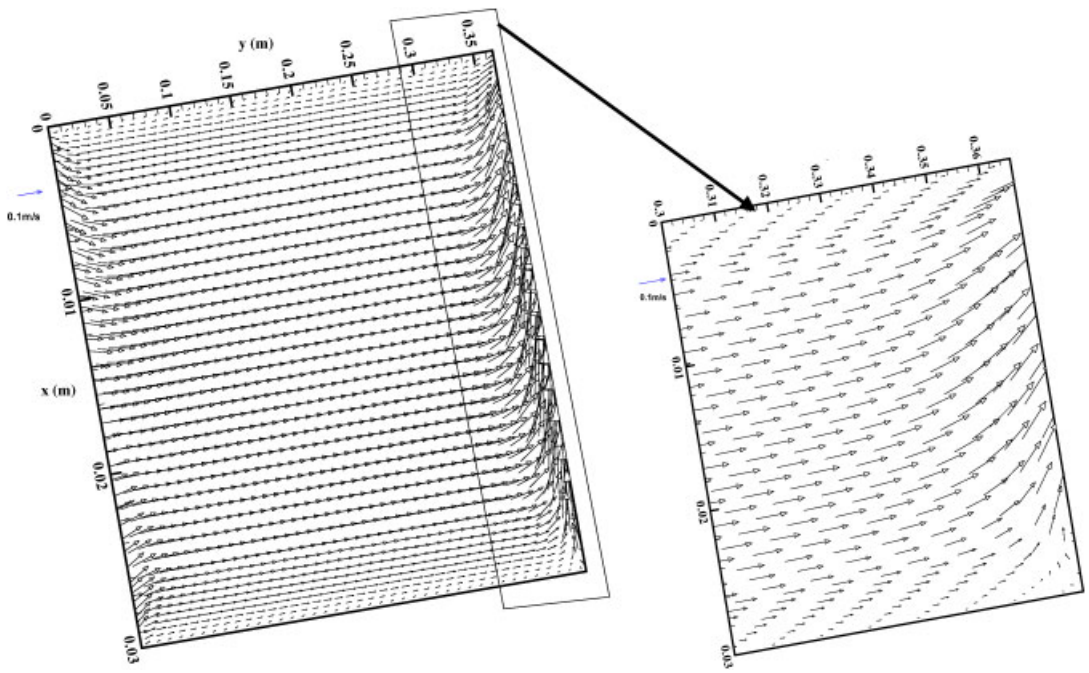

Figure 5. Velocity vectors for 80° inclination angle at $Ra' = 190$.

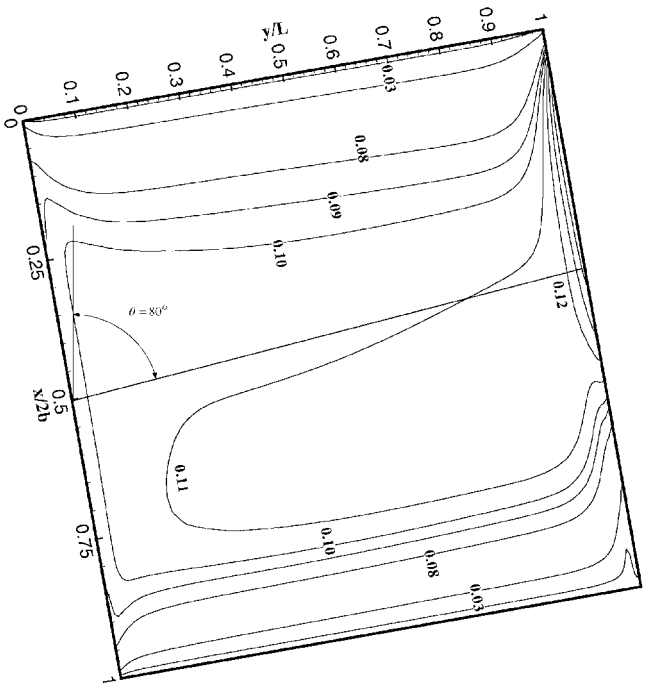

Figure 6. Velocity contours for 80° inclination angle for $Ra' = 190$.

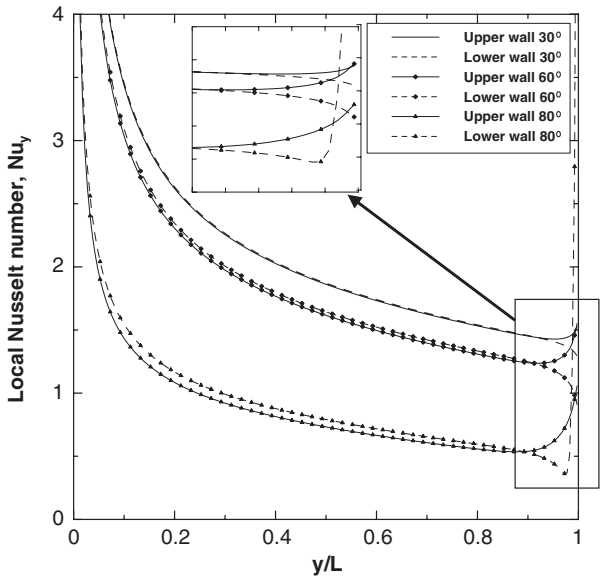

Figure 7. Local Nusselt number distribution along upper and lower walls for a modified Rayleigh number of 190.

the upper and lower walls in the direction of flow except at the channel exit where the effect of inclination becomes more significant. The local Nusselt number along the upper wall in the region close to the channel exit increases for all inclination angles. This is due to the increase in velocity gradients at the upper wall in the region close to the exit. On the other hand, the local Nusselt number along the lower wall in the region close to the channel exit decreases for inclination angles $\theta \leqslant 60°$. This decrease is due to the decrease in the velocity gradients along the lower wall in the region close to the channel exit. For the case of 80° inclination, the local Nusselt number increases sharply along the lower wall in the vicinity close to the channel exit. This sharp increase is caused by the large temperature gradient due to the reverse flow that takes place as shown in Figure 5.

The fifth set of results pertains to the effect of the inclination angle on the overall channel average Nusselt number. Figure 8 shows the plot of the average Nusselt number ($\overline{Nu}$) versus the modified $Ra(Ra' = Gr\,Pr\,b/L)$. As can be seen from Figure 8 the overall channel average Nusselt number decreases as the inclination angle increases. The rate of reduction increases as the inclination angle is increased at all values of Rayleigh numbers (Ra'). The amount of reduction is in good agreement with results reported by Straatman *et al.* [13] for the inclination angle range $0° \leqslant \theta \leqslant 30°$. It can also be observed that the rate of reduction decreases as the Rayleigh number (Ra') increases. As in the case of the vertical channel, the overall inclined channel average Nusselt number increases as the Rayleigh number (Ra') is increased. Figure 9 shows the plot of the overall channel average Nusselt number ($\overline{Nu}$) versus the product of the modified Ra' and the cosine of the angle of the inclination ($Ra' \cos\theta$) for the entire range of inclination ($0° \leqslant \theta \leqslant 80°$). As clearly shown in the figure, all the 10 curves plotted in Figure 8

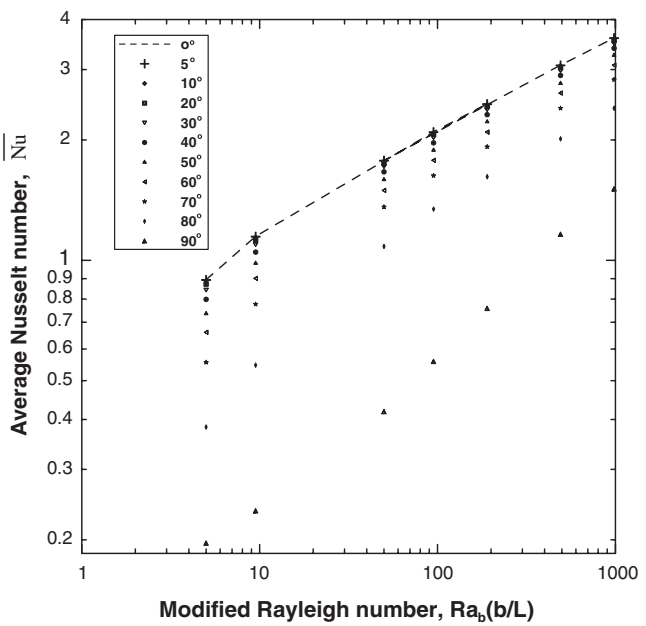

Figure 8. The overall channel average Nusselt number versus modified Rayleigh number for $0° \leqslant \theta \leqslant 90°$.

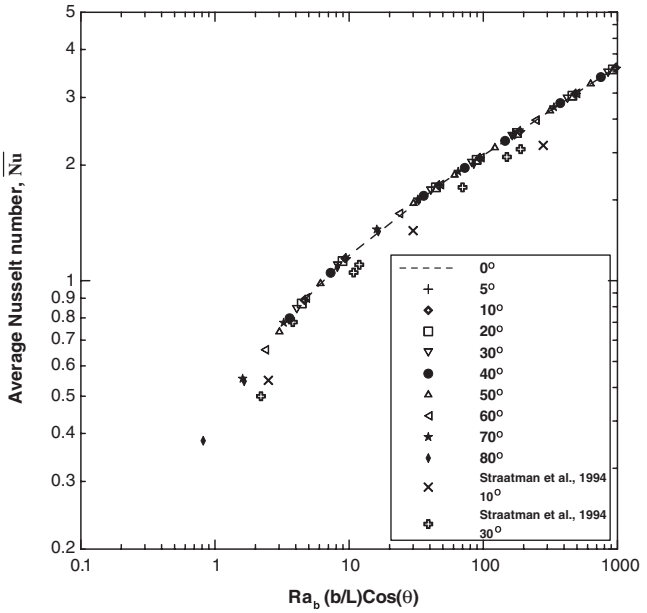

Figure 9. The overall channel Nusselt number versus the product of modified Rayleigh number and the cosine of angle of inclination ($Ra' \cos\theta$) for $0^\circ \leqslant \theta \leqslant 80^\circ$.

collapse to a single curve with no observable scatter. The product of $Ra' \cos\theta$ was used by Azevedo and Sparrow [11] and Straatman *et al.* [13] in correlations describing natural convection from inclined channels. In both Figures 8 and 9, the solid broken lines represent the vertical channel ($\theta = 0$) as a reference case. The results for the vertical channel were computed as part of the present study.

The sixth set of results pertains to the heat transfer characteristics of a horizontal channel (90° inclination angle). The velocity vectors plot Figure 10 indicate that cold air enters from both channel openings at the region close to the lower wall and hot air exits at the regions close to the upper wall. This results in a higher heat flux, and consequently a higher Nusselt number along the lower wall in comparison to the upper wall. The figure indicates two circulation zones having the middle section as a mirror image wall with an almost stagnant flow in the vicinity of the channel middle section. The results also indicate that as the Ra' increases; the size of the recirculation zone increases with the flow moving in almost parallel to the lower wall and out almost parallel to the upper wall and having minimum velocity values at around $x = b$. High velocity values appear at the channel middle section with the flow moving towards the upper wall.

The distribution of the local Nusselt number along the upper and lower walls for three values of Ra' of 190, 491 and 983 is shown in Figure 11. The figure indicates a reduction in the local Nusselt number in the direction towards the channel centre along the lower wall. The reduction in the local Nusselt number is attributed to the reduction in the velocity gradients in the region close to the upper and lower wall middle section for all values of Ra'. The same trend is found to occur along the upper wall for the case of $Ra' = 190$. As the Rayleigh

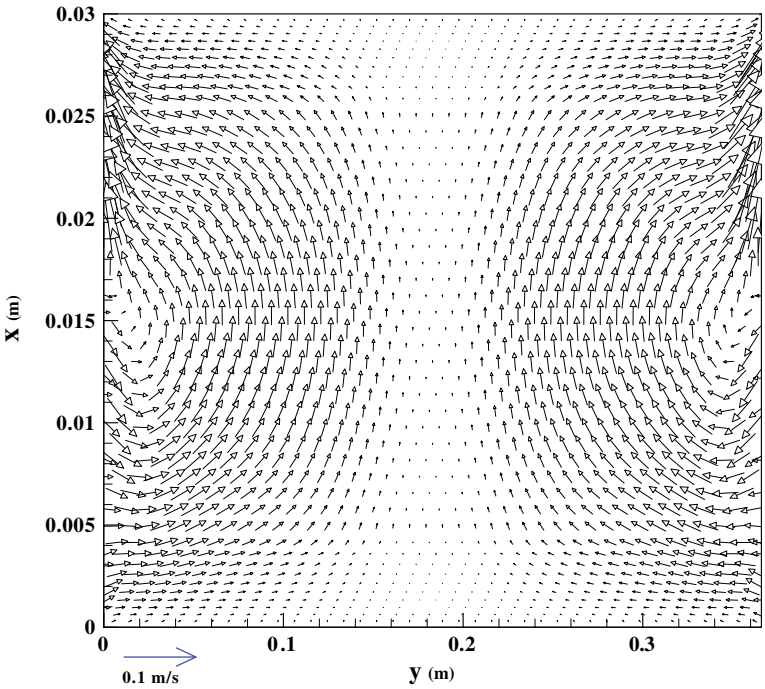

Figure 10. Velocity vectors for horizontal channel for $Ra' = 190$.

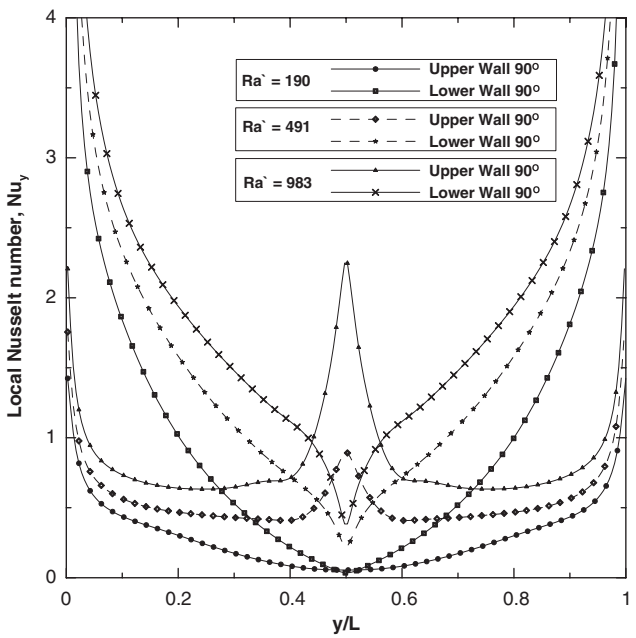

Figure 11. Local Nusselt number for horizontal channel at different values of $Ra'; \theta = 90°$.

number increases, the velocity of the flow entering from both channel openings increases and results in higher velocity gradients in the channel centre with a shift towards the upper wall as can be seen by the velocity vector plots shown in Figure 10. The increase in the local Nusselt number for higher Ra' in the vicinity of the upper and lower walls middle section is attributed to the increase in the velocity vector. As expected, the rate of increase is much higher along the upper wall. Figure 11 also indicates that the local Nusselt number is much greater along the lower wall in comparison to the upper wall at both channel openings.

5. CONCLUSION

The present study was carried out to investigate the effect of the angle of inclination (θ) on the heat transfer characteristics of a parallel-walled isothermal vertical channel. Velocity vectors, velocity and temperature contours and local and average Nusselt number results are presented graphically and discussed. The fluid flow results indicate that reverse flow regions are observed in the vicinity of the lower wall for inclination angles greater than 60°. The heat transfer results indicate that the local and average heat transfer decreases and that the rate of reduction increases as the angle of inclination is increased. The amount of reduction in the overall heat transfer due to the channel inclination is quantified by replotting them as a function of the product of a modified Rayleigh number (Ra') and the cosine of the angle of inclination ($\cos\theta$) for the range of inclination $0° \leqslant \theta \leqslant 80°$. Different trends are observed for the distribution of the local Nusselt number along the walls of the horizontal channel ($\theta = 90°$). The local Nusselt number, in the vicinity of the upper and lower wall middle section, increases as the Rayleigh number increases as a result of higher velocity gradients.

NOMENCLATURE

b	half channel width
C_p	constant pressure specific heat
g	gravitational acceleration
Gr	Grashof number $= (g\beta b^3(T_W - T_0)/\nu^2)$
h	average heat transfer co-efficient
h_y	local heat transfer co-efficient
k	thermal conductivity
L	channel length
Nu_y	local Nusselt number $= (h_y L/k)$
$\overline{Nu}$	average Nusselt number $= (hL/k)$
$\bar{P}$	dimensional pressure
Pr	Prandtl number
Ra	Rayleigh number $= (Gr\,Pr)$
Ra'	modified Rayleigh number $= (Ra\,(b/L))$
$\bar{T}$	dimensional temperature
T_O	ambient temperature
T_W	channel wall temperature

u, v x- and y-components of velocities, respectively
x, y Cartesian coordinates

Greek symbols

θ angle of inclination with respect to vertical
ρ density
α thermal diffusivity
μ dynamic viscosity
υ kinematic viscosity

Subscript

O refers to ambient

ACKNOWLEDGEMENTS

The authors would like to acknowledge the support of Mechanical Engineering Department, King Fahd University of Petroleum and Minerals for the present study.

REFERENCES

1. Elenbaas W. Heat dissipation of parallel plates by free convection. *Physica* 1942; **9**:1–28.
2. Bodia JR, Osterle JF. The development of free convection between heated vertical plates. *ASME Journal of Heat Transfer* 1962; **84**:40–44.
3. Aung W, Fletcher LS, Sernas V. Developing laminar free convection between vertical plates with asymmetric heating. *International Journal of Heat and Mass Transfer* 1972; **15**:2293–2308.
4. Kettleborough CF. Transient laminar free convection between heated vertical plates including entrance effects. *International Journal of Heat and Mass Transfer* 1972; **15**:883–896.
5. Oosthuzien PH. A numerical study of laminar free convective flow through a vertical open partially heated plane duct. *Fundamentals of Natural Convection-Electronic Equipment Cooling*, ASME HTD-vol. 32, 1984; 41–48.
6. Wirtz RA, Haag T. Effect of an unheated entry on natural convection between vertical parallel plates. *ASME Paper No. 85-WA/HT-14*, 1985.
7. Naylor D, Floryan JM, Tarasuk JD. A numerical study of developing free convection between isothermal vertical plates. *Transactions of the Journal of Heat Transfer* (ASME) 1991; **113**:620–626.
8. La Pica A, Rodono C, Volpes R. As experimental investigation on natural convection of air in a vertical channel. *International Journal of Heat and Mass Transfer* 1993; **36**:611–616.
9. Kihm KD, Kim JH, Fletcher LS. Onset of flow reversal and penetration length of natural convective flow between isothermal vertical walls. *Journal of Heat Transfer* 1995; **117**:776–779.
10. Hall DA, Vliet GC, Bergman TL. Natural convection cooling of vertical rectangular channel in air considering radiation and wall conduction. *Journal of Electronic Packaging*, *Transaction of the ASME* 1999; **121**(2): 75–84.
11. Azevedo LFA, Sparrow EM. Natural convection in open ended inclined channels. *Transactions of the Journal of Heat Transfer* (ASME) 1985; **107**(4):893–901.
12. Hajjai A, Warek WM. Analysis of combined fully-developed natural convection heat and mass transfer between two inclined parallel plates. *International Journal of Heat and Mass Transfer* 1988; **31**(9):1933–1940.
13. Straatman AG, Naylor D, Floryan JM, Tarasuk JD. A study of natural convection between inclined isothermal plates. *Journal of Heat Transfer* 1994; **116**:145–243.
14. Onur N, Aktas NK. An experimental study on the effect of opposing wall on natural convection along an inclined hot plate facing downward. *International Communications in Heat and Mass Transfer* 1998; **25**(3): 389–397.
15. Baskaya S, Aktas MK, Onur N. Numerical simulation of the effect of plate separation and inclination on heat transfer in buoyancy driven open channels. *Heat and Mass Transfer* 1999; **35**(44):273–280.
16. Bianco N, Morrone B, Nardini S, Naso V. Air natural convection between inclined parallel plates with uniform heat flux at the walls. *Heat and Technology* 2000; **18**(2):23–45.

17. Manca O, Nardini S, Naso V. Effect on natural convection of the distance between an inclined discretely heated plate and a parallel shroud below. *Transactions of the Journal of Heat Transfer* (ASME) **124**(3):441–451.
18. Jaluria Y. *Natural Convection Heat and Mass Transfer*. Pergamon Press: Oxford, 1980.
19. Fluent Inc. *Fluent Inc. Technical Manual*, 1998.
20. Patankar SV. *Numerical Heat Transfer and Fluid Flow*. Hemisphere Publishing Corporation: Washington, DC, 1980.
21. Versteeg HK, Malalasekera W. An introduction to computational fluid dynamics. *The Finite Volume Method*. Longman Scientific and Technical: New York, 1995.
22. Patankar SV, Spalding DB. A calculation procedure for heat, mass and momentum transfer in three-dimensional parabolic flows. *International Journal of Heat and Mass Transfer* 1972; **15**:1777–1787.
23. Choudhury D. Study of two benchmark heat transfer problem using FLUENT. ASME Heat Transfer Div. Publ. HTD, vol. 255, 21–30, *29th National Heat Transfer Conference*, 8–11 August 1993, Atlanta, GA, U.S.A.

